DR. SEAN J SHARP (Orcid ID : 0000-0002-6724-0186)

DR. WILLIAM S. CURRIE (Orcid ID : 0000-0003-1975-0808)

Article type : Articles

Journal: Ecological Applications

Manuscript type: Article

Running head: Flushing drives N cycling and invasion

Hydrologic flushing rates drive nitrogen cycling and plant invasion in a freshwater coastal wetland model

Authors: Sean J. Sharp[1*], Kenneth J. Elgersma[2], Jason P. Martina[3], William S. Currie[1]

[1]School for Environment and Sustainability, University of Michigan, 440 Church Street, Ann Arbor, MI, USA

[2]Department of Biology, University of Northern Iowa, 144 McCollum Science Hall, Cedar Falls, IA, USA

[3]Department of Biology, Texas State University, 601 University Drive, San Marcos, TX, USA

[*] Corresponding author: sjsharp@umich.edu

ABSTRACT

Coastal wetlands intercept significant amounts of nitrogen (N) from watersheds, especially when surrounding land cover is dominated by agriculture and urban development. Through plant uptake, soil immobilization, and denitrification wetlands can remove excess N from flow through water sources and mitigate eutrophication of connected aquatic ecosystems. Excess N can also change plant community composition in wetlands, including communities threatened by invasive species. Understanding how variable hydrology and N loading impact wetland N removal and community composition can help attain desired management outcomes, including optimizing N removal and/or preventing invasion by non-natives. By using a dynamic, process-based ecosystem simulation model, we are able to simulate various levels of hydrology and N loading that would otherwise be difficult to manipulate. We investigate *in silico* the effects of hydroperiod, hydrologic residence time, N loading, and the NH_4^+:NO_3^- ratio on both N removal and the invasion success of two non-native species (*Typha* x *glauca* or *Phragmites australis*) in temperate freshwater coastal wetlands. We found that when residence time increased, annual N removal increased up to 10-fold while longer hydroperiods also increased N removal, but only when residence time was >10 days and N loading was >30 g N m^{-2} y^{-1}. N removal efficiency also increased with increasing residence time and hydroperiod, but was less affected by N loading. However, longer hydrologic residence time increased vulnerability of wetlands to invasion by both invasive plants at low to medium N loading rates where native communities are typically more resistant to invasion. This suggests a potential tradeoff between ecosystem services related to nitrogen removal and wetland invasibility. These results help elucidate complex interactions of community composition, N loading and hydrology on N removal, helping managers to prioritize N removal when N loading is high or controlling plant invasion in more vulnerable wetlands.

Keywords: denitrification, ecosystem services, invasive species, nitrogen cycling, nutrient retention, *Phragmites australis*, residence time, *Typha* x *glauca,* wetland management

Introduction

Nutrient loads delivered to lakes and oceans have increased by orders of magnitude in the last half century, often due to changing land use or management practices in their watersheds, such as urban development and agriculture (Howarth et al. 2002). These large nutrient loads can lead to hypoxic dead zones (Diaz and Rosenberg 2008) and harmful algal blooms in receiving waters (Michalak et al. 2013, Lapointe et al. 2015) with consequences that reverberate from aquatic communities to local economies (Hoagland et al. 2002). Wetlands can provide services that mitigate impacts of elevated nutrient loading in some circumstances. For example, constructed wetlands are used as a tertiary treatment measure to remove large loads of nutrients from effluent (Kadlec and Wallace 1997) while wetlands along the paths of streams and rivers may sequester nutrients from the flow-through water (Knox et al. 2008). This has led many managers to optimize or expand nutrient removal in wetlands within their jurisdiction. However, conditions that improve nutrient removal may hinder other wetland functions and services, such as maintaining plant biodiversity or resisting invasive plant species (Hansson et al. 2005). Understanding the environmental conditions (e.g. water level or nutrient loads) that most influence certain wetland functions can help to optimize the most desired services while minimizing the sacrifice of others (Jessop et al. 2015).

Freshwater wetlands are widespread along lakeshores and in river channels and deltas, and many are hydrologically managed to influence water levels, wildlife habitat, or achieve other goals. In the Laurentian Great Lakes region of the Upper Midwest, USA, they are also widespread in coastal zones including river mouths and embayments. Because of their position on the landscape, these wetlands receive nutrient loads from surrounding water inflow (both upland runoff and open water fluxes) and can provide important nutrient removal services from these flow-through sources. Specifically, excessive nitrogen (N) loading can be ameliorated through important biotic pathways of removal, including plant uptake (Tylova-Munzarova et al.

2005), immobilization in litter and sediment organic matter (Vymazal 2007), and microbial transformation (e.g. denitrification; Jordan et al. 2015). However, excessive N loading to wetlands may also shift plant community structure, altering ecosystem function and potentially increasing vulnerability of plant communities to invasive species (Erwin 2009, Martina et al. 2016). In turn, the service of wetland N removal is likely to be affected by the interaction among N loading, plant growth and litter production, water levels, and hydrologic residence time (Pezeshki 2001). Given this complex set of interactions, understanding and managing N removal in wetlands is intrinsically challenging, especially when management goals are not complementary (Jessop et al. 2015).

N removal in wetlands is dominated by plant N uptake, immobilization in litter and sediments, and microbial denitrification, which are all controlled by various biotic and abiotic drivers. Removal via plant uptake and immobilization in soil occurs as plants assimilate inorganic N from porewater and overlying water to meet metabolic nutrient demands (Vymazal 2007). However, as plant detritus and soil organic matter decompose, organic N is subject to mineralization and rerelease in place or downstream as detritus and organic matter is flushed out of wetlands (Han et al. 2009). Unlike plant uptake and soil immobilization, denitrification (NO_3^--N transformation to gaseous N) is a more permanent removal pathway that occurs in anaerobic water and soil and is often coupled with aerobic nitrification, which converts NH_4^+-N to NO_3^--N (Reddy et al. 1989). Hydrology, through its control on anaerobic and aerobic conditions, is an important modulator of these N removal mechanisms. For example, hydroperiod determines the phasing and periodicity of aerobic and anaerobic cycles in wetlands which in turn control the rate of plant growth and N uptake by controlling soil anoxia (Reed and Cahoon 1992), the rate of litter decomposition, and whether aerobic nitrification or anaerobic denitrification is occurring (Ishida et al. 2006).

N removal is typically greater the more time N spends in wetlands and thus, in addition to hydroperiod, is also controlled by hydrologic residence time (henceforth, RT_h). RT_h modulates the contact time of N with microbes and plant rhizospheres for transformation and uptake, respectively (Kirk and Kronzucker 2005). The relationship of N removal and RT_h has been well studied in flow-through, constructed, and tertiary-treatment wetlands (Kadlec and Wallace 1997, Saunders and Kalff 2001, Ishida et al. 2006). Yet N removal in coastal wetlands is rarely studied (but see Dettmann 2007), in part due to the complex hydrology and N transport dynamics of

coastal zones. For example, water levels of the Laurentian Great Lakes fluctuate on decadal time scales, changing the hydrologic gradient from upland water sources to the Great Lakes, thus affecting water flow and RT_h of coastal wetlands that intercept these waters (Keough et al. 1999). Variable hydroperiods can further complicate our understanding of N removal in these wetlands. As soils alternate from aerobic to anaerobic with fluctuating water level, obligate aerobic and anaerobic processes change in tandem. The coincidence of fluctuating water levels with seasonal changes in temperature and plant productivity can lead to further complex interactions of N removal drivers. Finally, many N removal studies only focus on abiotic drivers, such as hydrology, and rarely incorporate biotic drivers or peripheral impacts to plant community structure despite well-known feedbacks between biotic and abiotic drivers (Corenblit et al. 2011).

In fact, plant communities have a powerful influence on nutrient cycling and soil biogeochemistry in wetlands, including the accumulation of nutrients stored in detritus (Weltzin et al. 2005). Likewise, greater nutrient availability can shift plant competition dynamics and plant community composition. For example, increased N loading can facilitate invasion of large-stature, non-native plant species that are better competitors for nutrients and light and deposit more litter than native competitors, thus increasing soil N pools and therefore N removal (Martina et al. 2016, Uddin and Robinson 2017). In particular, the success of *Phragmites australis* and *Typha* × *glauca*—both noxious, large-stature invaders of Great Lakes and other North American wetlands—is largely driven by increased N loading (Martina et al. 2016). Through superior competition for N and intraspecific N transfers within clones, these invaders can expand to the extent that they create near-monocultures in coastal wetlands (Zedler and Kercher 2004, Rickey and Anderson 2004). In facilitating these invasive plants, N availability likely interacts with other factors including nutrient cycling dynamics and hydrological disturbances (Wilcox 2012, Bansal et al. 2019). To improve our understanding of these complex drivers we need to examine how hydroperiod and RT_h of coastal wetlands interact to affect N removal and how changes in N removal will potentially alter the invasibility of wetland plant communities (Fig. 1).

Simulation models allow us to explore a wide range of these complex processes and interactions in thousands of structured scenarios and factorial combinations that would be difficult or impossible to perform in field studies. Here we examined *in silico* how RT_h,

hydroperiod, and N loading interact to affect N cycling and N removal rates in emergent wetlands, thereby influencing the outcomes of wetland plant invasions. We examine various hydroperiod frequencies with the same flooding range and total number of flooded days but with different flooding duration, in addition to wetlands with constant low and high water level. We also examined N loading with various nitrate (NO_3^-) to ammonium (NH_4^+) ratios as N removal and transformation processes can require one or the other species and because these ratios vary across the landscape (Hamlin et al. 2020; L Wan *pers comm*). We then assessed how these conditions influence N removal in two ways: annual N removal (i.e. the total N mass removed from an area in a given time) and N removal efficiency (i.e. N removed and denitrified relative to N entering wetlands).

We simulated a range of these hydrologic and nutrient cycling variables in scenarios where one of two non-native invasive graminoids (*Phragmites australis* or *Typha* × *glauca*) was introduced into an established native plant community typical of Great Lakes coastal wetlands using Mondrian, a process-based model of wetland ecosystems that includes plant competition and dynamic community change over time. We hypothesized that longer RT_h would increase the percent of N inflow denitrified, while N loading dominated by NH_4^+ would limit denitrification, resulting in less overall N removal (Fig. 1, H_1). Second, we hypothesized that, assuming the total number of flooded days is equal, simulated wetlands with longer hydroperiod would result in less annual denitrification and subsequent N removal (Fig. 1, H_2). When wetlands flood and draw down often, aerobic nitrification, which transforms NH_4^+ to NO_3^-, can also occur more frequently replenishing depleted stocks for denitrifying microbes compared to less frequently flooded wetlands. Finally, in scenarios of long RT_h whereby N inflow exceeds N outflow, we hypothesized that higher levels of plant-available inorganic N would drive the success of wetland plant invasion and subsequently increase N uptake and ecosystem N removal due to the high N demands of these large-stature invaders (Fig. 1, H_3). We demonstrate the potential for a novel ecosystem tradeoff between N removal and invasion risk driven by RT_h in freshwater coastal wetlands.

Materials and methods

Mondrian Simulation Model

We used an individual-based, spatially-explicit wetland ecosystem model, Mondrian, which spans multiple levels of ecological organization from individual plant physiology to

population, community, and ecosystem processes. The model was previously developed to study N cycling and plant invasion (Currie et al. 2014, Martina et al. 2016, Elgersma et al. 2017, Goldberg et al. 2017). We give a brief overall description with some detail on processes and functions either newly added or key to understanding the present study.

Mondrian utilizes a grid space that can be divided into ≤ 625 cells. Over this framework of grid cells, a user-defined number of individual propagules (i.e. ramets) are stochastically dispersed. Individual ramets have defined, species-specific traits, including relative growth rate, maximum plant size and tissue nutrient requirements. Ramets within grid cells compete for available N and light within the same cell (for details on light competition see Martina et al. 2016). Plants clonally reproduce, spreading rhizomes stochastically through the model space, and share resources via translocation among rhizome chains. The modeled substrate is vertically organized with mineral soil organic matter (MSOM) on the bottom, then muck, and aboveground litter on top. Although the thickness of the MSOM layer is fixed (30 cm), the thicknesses of the muck and litter pools vary depending on relative rates of litter production and decomposition, allowing accretion or subsidence of the muck surface. At the ecosystem level, the user defines daily N inflow, daily water level and water flow rate, daily temperature, and growing season length. Several ecosystem processes emerge from these fine-scale processes, including plant productivity, community composition, and C and N cycling dynamics. The model has balanced C and N cycles and explicitly represents and tracks ecosystem C and N stocks, export, transformation, and removal (defined below).

In this study, we introduce an updated version of Mondrian (version 4.3) parametrized for wetlands of the Great Lakes region with improved realism in certain aspects of clonal plant growth and N cycling. The updated model simulates lateral and terminal branching of rhizomes in clonal plants (see Martina et al. *in prep.* for full description), and now includes flooding-induced mortality for individual plants. It also explicitly partitions available NH_4^+-N and NO_3^--N, includes inflow and export of each separately, and includes nitrification and denitrification processes (described below). Finally, the modified model allows flexibility in the inflow and hydrologic flushing rate of N, which can be constant or vary daily.

Nitrification and denitrification

N cycling in Mondrian has been augmented to include coupled nitrification and denitrification, the latter providing an additional N removal pathway. In previous model versions, N that was not taken up by plants or immobilized in detritus was flushed out of the wetland at a certain rate, the balance remaining as plant-available N. We calculate nitrification and denitrification as daily fluxes (g N m^{-2} day^{-1}) spatially explicit within grid cells, using equations (1) and (2), respectively.

$$Daily\ nitrification\ (g\ N\ m^{-2}\ day^{-1}) = l_{amm} \cdot f_{aer}(NH_4^+) \cdot f(T_{soil}) \cdot \theta_n \quad (1)$$

$$Daily\ denitrification\ (g\ N\ m^{-2}\ day^{-1}) = l_{nitr} \cdot f_{ana}(NO_3^-) \cdot F_{resp} \cdot \theta_d \quad (2)$$

where, l_{amm} and l_{nitr} represent grid cell NH_4^+-N and NO_3^--N pools (g N m^{-2}), respectively, and $f(T_{soil})$ represents the effect of soil temperature. In Mondrian, we assume that for any soil above a defined water level height, soil temperature (T_{soil}) is equal to ambient air temperature and T_{soil} of any flooded soil below this water level equals the temperature of the overlying water. As nitrification requires aerobic conditions and denitrification requires anaerobic, these processes are constrained by the terms $f_{aer}(NH_4^+)$ and $f_{ana}(NO_3^-)$, which represent the proportion of l_{amm} that is aerobic and l_{nitr} that is anaerobic, respectively. Unlike nitrification, which involves oxidizing ammonia (NH_4^+) to nitrate (NO_3^-) and is modulated by $f(T_{soil})$, denitrification is a heterotrophic process and involves the oxidation of labile soil organic C. Heterotrophic respiration, including the effects of temperature and the size of detrital pools, is already included in Mondrian. Therefore, F_{resp}, a unitless factor that tracks rates of soil heterotrophic respiration, conveys a temperature effect and tracks substrate availability for denitrifying microbes in a similar fashion as other denitrification models (Parton et al. 1996). Finally, the model was calibrated (described below) to ecosystem-scale observations using scaling parameters for both nitrification (θ_n) and denitrification (θ_d).

Nitrification and denitrification occur in the model within explicit vertical limits we refer to as the 'active zone' for each process. This allows us to calculate, based on daily water level, which proportion of the active zone is aerobic and anaerobic. The top of the vertical active zone is defined as the top of the muck layer for denitrification, and for nitrification extends up to 5 cm into the aboveground litter layer above the muck where conditions are likely to be more aerobic than in muck and MSOM, even when flooded. For this study, the lower boundary of the active zone is set to 5 cm depth in the mineral soil, below which the rates for both processes have been

observed to be negligible (Brodrick et al. 1988). Any detrital pool (or partial pool) below a 5-day trailing average of water level is anaerobic in the model, but these pools become aerobic when above the water level on a daily basis. Mondrian does not include nitrification or denitrification in the overlying water column. At temperatures below 4°C, rates of nitrification and denitrification are assumed to be negligible (Bremner and Shaw 1958).

To calibrate the ecosystem-level scaling parameters (θ_n and θ_d) we used 5 sentinel sites from the Great Lakes region with observational data for multiyear data sets of *in situ* denitrification. We only included studies with field measurements of denitrification (i.e. measured fluxes of $N_2 + N_2O$) and omitted studies that measured only potential denitrification in ideal laboratory settings or with an augmented supply of nitrate. We simulated the relevant conditions reported at each sentinel site in Mondrian, including annual average temperature, temperature range, growing season length, water level, N inputs, and plant community (Table 1). For sites that did not report both NH_4^+ and NO_3^- inputs, we used a 1:3 ratio of NH_4^+-N:NO_3^--N, typical of land use dominated by high intensity agriculture in which these sites were situated (Hamlin et al. 2020). We then adjusted both θ_n and θ_d to achieve a best fit using a residual sum of squares (Fig. 2).

Simulated experimental design

We used 5 hydroperiods, 5 RT_h, 6 levels of N loading, 5 N species ratios, and 2 invasion scenarios amounting to 1380 unique combinations of these factors (Table 2). Here we describe each of these factors in turn. In Mondrian, hydroperiod is controlled by defining water level daily. In these simulations we used 5 hydroperiods, including permanently flooded (water level +15cm in relation to the MSOM soil horizon), permanently exposed (water level -15cm), and sinusoidal fluctuating water level (±50 cm) with weekly, monthly or semi-annual periodicity. These fluctuating hydroperiods reflect weather events that occur on short (weekly) and medium (monthly) time scales and seasonal (semi-annual) fluctuations that occur on a longer time scale with water level peaking in mid-June. All wetlands with variable hydroperiod in these simulations (weekly, monthly, and semi-annual) experienced the same maximum flooding depth and total number of days with overlying surface water per year with the only difference being the timing of flooding.

In Mondrian, the proportion of the NH_4^+-N and NO_3^--N pools exported daily from the wetland is controlled by a hydrologic flushing parameter, which equals the inverse of hydrologic residence time (RT_h). Daily values of RT_h and water level are read in from an input file, allowing simulation of seasonal hydrological trends. For this study, we modeled RT_h either as a fixed rate throughout the simulation (four scenarios independent of water level) or as a function of water level (three scenarios). For fixed rates, we chose RT_h values of 1, 10, 100 and 365 days to capture a range of wetland types found in the Great Lakes region, from a small, flow-through wetland to a coastal embayment with a one-year residence time, respectively (Morrice et al. 2004). In our scenario where RT_h is a function of water level we used an exponential relationship

$$RT_h = \frac{1}{ae^{bh}} \quad (3)$$

where a and b are constants, h is water level (m), and where lower water level corresponds to longer RT_h. To parameterize the constants a and b, when water level was lowest we used RT_h = 365 d and when water was highest we used RT_h = 1 d. Under constant water level scenarios of permanently flooded and permanently exposed, RT_h as a function of water level would also be constant. Therefore, these scenarios are omitted as a treatment combination, leaving only weekly, monthly, and semi-annual hydroperiods with RT_h as a function of water level.

In addition to hydroperiod and RT_h, we used 6 levels of N-loading, ranging from oligotrophic, precipitation-fed wetlands (1 g N m^{-2} y^{-1}) to highly eutrophic wetlands (100 g N m^{-2} y^{-1}; Krieger 2003). We then partitioned the 6 levels of N-loading into NH_4^+-N and NO_3^--N proportions that included conceptual NH_4^+-only or NO_3^--only N inputs as end points, together with three NH_4^+-N:NO_3^--N ratios that characterize wetland N loading from three dominant land use classes in the region: urban (1:7.3), high-intensity agriculture (1:3), and rural (4:1; Hamlin et al. 2020). Finally, we simulated plant communities in which either *Phragmites australis* or *Typha x glauca*, two common invasive species in the Great Lakes region, are introduced into established communities comprising three native wetland species: *Eleocharis smallii, Juncus balticus,* and *Schoenoplectus acutus*. At year 15, after the native community has reached a steady-state density, we introduce a cohort of 15 individual ramets of one of the two invasive species and introduce another identical cohort 5 years later. A background colonization rate of 1 ramet per year per species continues for all species after initial introduction into the modeling space.

Each of the 1380 combinations was run for 55 years, enough time for the simulation to achieve ecosystem stability, with 3 stochastic replications. Mondrian outputs large amounts of data after each model run ranging from stem density to total ecosystem C. For this study, we averaged all output of the last 5 years of each simulation (years 51-55) to integrate across inter-annual variation. We limited the response variables we examined to annual N removal (g N m^{-2} y^{-1}), percent denitrification (%), N removal efficiency (%), and invader percentage of community NPP (%). To account for the large disparity between denitrification rates under low and high N loading, we interpreted denitrification as the percentage of annual N inflow denitrified. We define annual N removal (N_{rem}) as

$$N_{rem} = N_{in} - N_{out} \quad (4)$$

percent denitrification (N_{dntr}) as

$$N_{dntr} = \frac{Annual\ denitrification\ (g\ N\ m^{-2}\ y^{-1})}{N_{in}\ (g\ N\ m^{-2}\ y^{-1})} \quad (5)$$

and N removal efficiency as

$$N\ removal\ efficiency = \frac{N_{rem}}{N_{in}} \quad (6)$$

where N_{in} is the sum of annual N inputs, including annual surface N loading and atmospheric N deposition and N_{out} includes the annual hydrologic export of all NO_3^--N, NH_4^+-N, and detritus-bound organic N.

Statistical analysis

We used Generalized Linear Mixed Models (GLMM) to examine the effects of treatment combinations of predictor variables, including N loading, NH_4^+-N:NO_3^--N ratio, RT_h, hydroperiod, and plant invader species (Table 2) on total annual N removal, N removal efficiency, percent of annual N inflow denitrified, and invader proportion of community NPP response variables averaged over the last 5 years of simulations (Bates et al. 2015). N loading and RT_h were analyzed as continuous numeric variables and NH_4^+-N:NO_3^--N ratio, hydroperiod, and plant invader species as factors with discrete levels. When RT_h was a function of water level, we used the average annual RT_h ($RT_h \approx 4$ days) to include this treatment within the range of other continuous RT_h values (see Figs. 3-5). To develop a best-fit GLMM, we used a forward stepwise algorithm in which terms are iteratively added, starting from a null model lower bound to a global model (i.e. a model including all main effects and their possible interactions) upper

bound. This algorithm uses Akaike Information Criterion (AIC) to select the best GLMM by scoring each model based on goodness-of-fit and model parsimony, only adding more terms when such additions improve the AIC value. In addition to ranking models based on AIC and goodness-of-fit (adjusted R^2), we also ranked terms within each best fit GLMM by their relative variable importance (RVI) value (Burnham and Anderson 2002) to focus our analysis to only the most important main effects and interactions, despite other main effects and interactions also being important, albeit less so (Table 4). RVI values are calculated by summing the Akaike weights, a goodness-of-fit measure of a single model weighted across an array of models, for all possible GLMMs in which a given variable occurs. Because RVI values of main effects and interactions are relative they cannot be directly compared to one another (e.g. RVI values of two-way interaction terms can only be compared to RVI values of other two-way interaction terms and not with RVI values of main effects or higher order interactions), we interpret these terms separately. All data were analyzed using the "lme4" (Bates et al. 2015) and "MuMIn" (Barton 2019) packages in the statistical computing software R version 3.6.1 (R Core Team 2019).

Results

In our simulations of Great Lakes coastal wetlands, we found that hydrologic residence time (RT_h), hydroperiod, and N loading were all strong predictors of wetland N removal, including annual N removal, N removal efficiency, and percent denitrification (Tables 3 and 4). Furthermore, these drivers interacted such that N removal was greatest when RT_h and hydroperiod were longest, yet each measure of N removal was affected differently by changes in N loading (Figs. 3-6). Drier wetlands (e.g. wetlands with constant low water) had a limited capacity for N removal compared to flooded wetlands in our simulations. As plant litter and organic matter pools became aerobic, denitrification stopped, decomposition was accelerated, and mineralized N was exported downstream. Alone, NH_4^+-N:NO_3^--N ratio and plant invader identity had little influence on any measure of N removal, but when interacting with N loading were important predictors of annual N removal. Under semi-permanent flooding, N removal was greater when N loading had a higher proportion of NO_3^- compared to N loading with a higher proportion of NH_4^+ (Fig. 7). Under high N loading, in communities where *Typha* was introduced but failed to establish, slightly more N was removed annually compared to *Phragmites*-invaded communities. Finally, although invader identity was an important predictor of invasion success,

which, like N removal, was driven by RT_h, N loading, and less so, hydroperiod, it was less important in predicting wetland N removal.

Due to the similarity in outcomes of several treatment levels and in an effort to simplify the presentation of results, we dropped several treatment levels from figures, but still included them in all analyses. We chose a single land use-derived NH_4^+-N:NO_3^--N ratio, 1:3 (representing high-intensity agriculture, the most dominant land cover in the region) because N species ratios had negligible effects in most scenarios. We omitted non-flooded wetlands where N removal was always very low, and combined results from wetlands with permanent and semi-annual hydroperiods (hereafter referred to as semi-annual), which always had similar responses to each other. We also omitted the lowest N loading scenario (1 g N m^{-2} y^{-1}), and only present low (5 g N m^{-2} y^{-1}), medium (30 g N m^{-2} y^{-1}), and high (100 g N m^{-2} y^{-1}) N loading treatments.

Annual N removal

We assessed N removal in either absolute terms of annual N removal (g N m^{-2} y^{-1}) or relative terms of N removal efficiency (i.e. N removed and denitrified relative to N entering the wetland). Annual N removal (including soil immobilization, plant uptake, and denitrification; Figs. 3 & 5), N removal efficiency (Fig. 6), and percent denitrification (i.e. % of N inflow denitrified; Fig. 7) generally increased with longer RT_h, but N loading and RT_h interacted with hydroperiod such that N removal was greatest with longer hydroperiod only under certain combinations of N loading and RT_h. Permanently exposed wetlands exhibiting very low annual N removal as organic N in the soil quickly mineralized (data not shown) and microbes were unable to denitrify under aerobic conditions. Annual N removal (Fig. 3) increased most with increasing N loading (5-100 g N m^{-2} y^{-1}) and RT_h (1-365 days). However, only under high N loading (100 g N m^{-2} y^{-1}) and RT_h >10 days did longer hydroperiod (weekly to semi-annual) result in a notable increase (>10 g N m^{-2} y^{-1}) in annual N removal. In wetlands with N loading of 30 and 100 g N m^{-2} y^{-1}, as RT_h increased from 10 to 100 days annual N removal increased nearly 10-fold while in wetlands with low N loading annual N removal was relatively unaffected by RT_h. In addition to RT_h, hydroperiod, and N loading and their interaction, the interactions of NH_4^+-N:NO_3^--N ratios with these main effects were also important predictors of annual N removal (Table 4). Wetlands with semi-annual hydroperiod and N loading dominated by NH_4^+ had lower annual N removal compared to wetlands with other N loading ratios because without NO_3^- or the aerobic conditions

needed to transform NH_4^+ to NO_3^- in these wetlands, denitrification was arrested (Fig. 4). Invader identity only affected annual N removal under high N loading (100 g N m^{-2} y^{-1}), with native communities where *Typha* was introduced but failed to establish removing approximately 5 g N m^{-2} y^{-1} more N than *Phragmites*-invaded communities, a relatively small increase when compared to the differences resulting from longer hydoperiod (>10 g N m^{-2} y^{-1}) and longer RT_h (>60 g N m^{-2} y^{-1}; Fig. 3). However, at lower rates of N loading, annual N removal was similar across both communities.

The dominant mechanism of N removal in our simulations was uptake by plants and subsequent deposition of plant litter into soil pools, where under anaerobic conditions it accumulates, resulting in the largest N pool in the wetland (soil organic N; Fig. 5). As the major contributor to annual N removal, soil organic N pools similarly increased with longer RT_h, greater N loading, and longer hydroperiod. In particular, soil organic N was limited by aerobic conditions from weekly flooding while semi-annually flooded conditions allowed larger soil organic N pools to accumulate. Plant uptake also increased with RT_h and N loading but was not constrained by hydroperiod. Plants and soil pools became somewhat N saturated under N loading of 30 g N m^{-2} y^{-1} when RT_h was ≥10 days and across all levels of RT_h under N loading of 100 g N m^{-2} y^{-1} as soil N pools and N uptake plateaued (Fig. 5).

N removal efficiency increased from 6% to 74% under higher N loading as RT_h increased from 1 to 365 days, was slightly higher under longer hydroperiods (Fig. 6). Yet under low N loading (5 g N m^{-2} y^{-1}), N removal efficiency reached only 62% when RT_h was longest. Similar to annual N removal, in semi-annually flooded wetlands N removal efficiency was only affected by high NH_4^+-N:NO_3^--N ratios in which denitrification was arrested (Appendix S1: Fig. S1) .In wetlands with short RT_h (1-10 days), N removal efficiency was consistently low when N loading was high (100 g N m^{-2} y^{-1}), unlike wetlands with N loading <100 g N m^{-2} y^{-1} where efficiency steadily increased with increasing RT_h.

Percent denitrification only increased with high N loading (30-100 g N m^{-2} y^{-1}) and longer RT_h (100-365 days; Table 3, Fig. 7). In addition, wetlands with semi-annual hydroperiod denitrified up to 10 g N m^{-2} y^{-1} more than weekly flooded wetlands and percent denitrification increased from <1% to 69% as RT_h and N loading increased (Fig. 7). The NH_4^+-N:NO_3^--N ratio affected denitrification rates only in wetlands with longer, semi-annual hydroperiod where obligate-aerobic nitrification was inhibited (Appendix S1: Fig. S1). Under semi-annual

hydroperiod, as N loading became dominated by NH_4^+-N, denitrification decreased by as much as 89% under high N loading compared to N loading dominated by NO_3^--N (Appendix S1: Fig. S1) and was negligible (<0.02 g N m^{-2} y^{-1}) under low N loading

Community invasion

Invasion was mostly driven by N availability and was even successful under the lowest N loading scenario as longer RT_h resulted in large enough pools of plant-available N to facilitate the dominance of both *Phragmites* and *Typha* over native plant communities (Figs. 4-6; Appendix S1: Fig. S2). Although invader identity was an important predictor of invasion success (measured by invader % NPP of community NPP), with *Phragmites* a more successful invader than *Typha*, it was not an important predictor of N removal (Table 4). A 3-way interaction of invader identity, N loading, and RT_h was also an important predictor of invasion success (Table 3). As RT_h and N loading increased, native communities became increasingly invader dominated, but only up to N loading of 10 g N m^{-2} y^{-1}, above which *Phragmites* invasion occurred regardless of RT_h and *Typha* invasion occurred only with shorter RT_h.

Under the lowest N loading regime (1 g N m^{-2} y^{-1}), *Phragmites* successfully invaded plant communities (i.e. >75% community NPP) in non-flooded, permanently exposed wetlands with RT_h >100 days, but failed to establish in any flooded wetlands, regardless of RT_h (Appendix S1: Fig. S2). Yet with each increasing level of N loading and RT_h, *Phragmites* % of NPP also increased. At N loading of 30 g N m^{-2} y^{-1}, wetlands communities were nearly 100% invaded by *Phragmites* at even the shortest RT_h (1 day). At N loading of 5 g N m^{-2} y^{-1}, *Phragmites* invasion was successful at RT_h of 10 days and at 15 g N m^{-2} y^{-1} was successful at RT_h of only 1 day (Appendix S1: Fig. S2).

Typha invasion, however, was successful only in discrete ranges of N loading and RT_h. *Typha* comprised >75% of community NPP at 5-10 g N m^{-2} y^{-1} when RT_h was longest (100 and 365 days) and at 15 g N m^{-2} y^{-1} when RT_h was 4 to 10 days long (Appendix S1: Fig. S2). *Typha* invasion was also successful when N loading was 30-100 g N m^{-2} y^{-1} and RT_h was shorter (1 to 10 days). In scenarios where plant-available N was abundant, yet in which *Typha* did not successfully invade, we observed *Schoenoplectus acutus,* a large-stature native plant, would grow quickly, reaching high NPP similar to a *Typha*-dominated community (ca. 1750 g C m^{-2} y^{-1}). *S. acutus* would fill the model space before year 15 when invaders are introduced in our

model, effectively resisting invasion. This mechanism of resistance was confirmed with a set of diagnostic model simulations (Appendix S1: Fig. S3) in which *Typha* was either introduced at year one (rather than year 15), introduced with an equal number of propagules as native species (65 propagules rather than 15), or both (introduced on year 1 with 65 propagules). Only in scenarios in which *Typha* was introduced on year one with 65 propagules did it successfully establish and dominate native communities.

Discussion

Our model findings suggest that while annual N removal increased with both longer RT_h and increasing N loading, N removal efficiency most significantly increased with longer residence time (RT_h). Furthermore, under high N loading the increase in N removal efficiency with increasing RT_h only occurred in the 100-365 day range. Under low N loading (1-15 g N m^{-2} y^{-1}) these same drivers of N removal also facilitated the invasion of *Phragmites australis* and *Typha* x *glauca*. Specifically, we find that longer RT_h can result in an accumulation of N in simulated wetlands that provides more substrate for microbial transformation, like denitrification, and ample nutrients for plants to quickly grow and colonize. This introduces a potential trade-off of ecosystem N removal services and wetland invasion control, whereby hydrologic drivers that facilitate more N removal are also more likely to decrease resistance to invasion by *Phragmites* or *Typha*. Furthermore, these simulations help elucidate complex interactions of hydrology, N loading, and community composition on wetland N removal. As we demonstrate a potential tradeoff between N removal and wetland invasibility, we also present practitioners with information to help prioritize management objectives in coastal wetlands that are receiving large amounts of N or are at risk of invasion. However, these simulation results should be interpreted cautiously.

Although Mondrian incorporates many complex interactions across several levels of ecological organization, it offers only a functional representation of wetland ecosystems. Mondrian does not include every meaningful mechanism and driver of N removal and invasion in these environments and users should understand the assumptions and limitations of the model before using it as a decision-making tool. For example, in Mondrian the aerobic-anaerobic boundary occurs along a very discrete soil horizon at the top of the water table below the soil surface. In fact, anaerobic conditions and denitrification are known to occur in the overlying water column and be heterogeneous across soil porespace regardless of water table position

(Piña-Ochoa and Álvarez-Cobelas 2006, Kjellin et al. 2007). Therefore, Mondrian likely underestimates N removal via denitrification and managers should consider this in their decision making (Table 1; Fig. 2).

Furthermore, Mondrian does not explicitly model all plant-soil and plant-hydrology interactions, including (but not limited to) gas transport through plant stems, modulation of the rhizosphere environment, plant transpiration, and the drag imposed by vegetation on flowing water. Yet, these mechanisms can be important drivers of N removal processes which should be accounted for when interpreting Mondrian output (Reddy et al. 1989, Chanton and Whiting 1996, Kröger et al. 2009). For example, soil oxygen levels may increase where stem density is high or because of the physiology of particular species, feedbacks which Mondrian does not explicitly model (but that can be accounted for when calibrating the model with empirical data), potentially leading to an underestimation of the proportion of soil that is aerobic. Finally, transpiration and the drag vegetation imposes on flow-through water, important plant-hydrology interactions, are not included in Mondrian but are known to effect water level and RT_h, respectively (Sánchez-Carrillo et al. 2004, Kröger et al. 2009). However, Mondrian does allow for user-defined, daily changes in water level and RT_h to account for these effects. Despite these limitations, the effect size of RT_h and N loading on N removal and plant invasion is large enough to support use of the general patterns presented in this study to inform wetland management across the region and other freshwater coastal wetlands affected by variable hydrology and N loading.

N removal, RT_h, and denitrification

Inorganic N inputs are initially retained in wetlands through immobilization in microbial communities or assimilation in plants. Annual N removal, which combines plant uptake, soil immobilization, and denitrification, generally increased with more N loading and longer RT_h. Yet at higher N loading both annual N removal and N removal efficiency remained low at RT_h of 1-10 days as soil and plants became N saturated, N was flushed out faster, and there was less N contact time for denitrifying microbes. Surprisingly, under long RT_h (100-365 days), N loading of 100 g N m^{-2} y^{-1} was just as efficient at N removal as wetlands under lower N loading. However, this also indicates that wetlands with high N loading require very long RT_h to be effective at N removal. Supporting our hypothesis and similar to other model analyses (e.g.,

Dettmann 2007), we found that longer RT_h also increases rates of denitrification. As RT_h increases, the flushing of N out of the system slows, causing it to accumulate in the wetland (Perez et al. 2011). Increases in available N pools supply more N substrate for transformation by denitrifying microbes. Similarly, longer RT_h in the wetland creates more opportunity for plant uptake, thus increasing N removal compared to scenarios with shorter RT_h.

Invader identity had little impact on denitrification in our simulation, despite being recognized as an important driver in field studies (Findlay et al. 2003). For example, compared to native plants, *Phragmites* provides more labile organic carbon to soil providing energy subsidies for microbes and more oxygen to the rhizosphere which facilitates nitrification in coupled nitrification-denitrification N removal (Windham and Meyerson 2003, Ehrenfeld 2003). Although Mondrian does include subsidies of organic carbon, it does not explicitly model gas transport in plants and this may result in underestimates of denitrification in our simulations. However, the influence of *Phragmites* in particular can be highly variable (Alldred and Baines 2016), and likely driven by small scale variation at spatial resolutions outside the limits of our model. Furthermore, only a small portion of N removal in our studies was attributed to denitrification suggesting the impacts of *Phragmites* on denitrification does not affect the overall patterns of N removal we observed.

Annual N removal was affected by hydroperiod only in extreme scenarios (e.g. non-flooded vs. permanently flooded wetlands). More frequent flooding and shorter hydroperiods did not result in significantly higher percent denitrification as we predicted. Rather, percent denitrification was highest when hydroperiod was longest (e.g. semi-annual), although this difference was marginal compared to the large effects incurred by changes in RT_h (Fig. 5). We believe this is due in part to the seasonal timing of flooding in these simulations, a known driver of denitrification and other wetland processes (Valett et al. 2005, Langhans and Tockner 2006). Although wetlands with weekly hydroperiod were flooded the same total number of days in a year as wetlands with semi-annual hydroperiod, flooded conditions in semi-annual wetlands were concentrated in the growing season (water level peaks during June) when soil temperature is high and microbes are most active. In other words, denitrification conditions were near optimal for all flooded days in semi-annual wetlands but only half the flooded days when hydroperiod was weekly, the other flooded days being too cold for denitrification to occur. Only when NO_3^- was scarce (i.e. when NH_4^+-N:NO_3^--N ratios were high) did wetlands with weekly hydroperiod

have higher percent denitrification than wetlands with semi-annual hydroperiod (Fig. 5). In these scenarios, NO_3^- is limiting and frequent shifts to aerobic soil conditions facilitate oxygen-dependent nitrification, transforming NH_4^+ to NO_3^- needed for denitrification.

Indeed, others have found that under high inputs of NO_3^-, wetlands with longer, less variable hydroperiods removed more N and had higher rates of denitrification than wetlands with more variable, shorter hydroperiods (Ishida et al. 2006). Compared to drier wetlands or wetlands with shorter hydroperiod, wetlands with semi-annual hydroperiod remove and store more N as anaerobic conditions slow decomposition of plant litter and mineralization of organic N (Fig. 3). Decomposition and N mineralization are also slowed by low temperatures. Yet unlike denitrification, N removal via burial of N is less permanent and is more sensitive to changes in oxygen availability and temperature, especially as water levels draw down, or as organic matter is flushed downstream where it may be mineralized later in more oxygen rich waters (Venterink et al. 2002). Nonetheless, organic N stocks were higher in wetlands with longer hydroperiods, subsidizing overall N removal.

Plant invasion

In addition to increasing N removal, we found that longer RT_h also increases invasion success of *Phragmites australis* and *Typha* x *glauca.* While it was previously known that there was a threshold of invasion (~15 g N m^{-2} y^{-1}) across a N loading gradient for these two species (Martina et al. 2016), it was unknown that this threshold would be sensitive to RT_h. As RT_h increases, thresholds of successful *Phragmites* invasion shifted towards lower N loads, with invasion occurring even under the lowest N load we simulated (1 g N m^{-2} y^{-1}). When RT_h is longer, N is flushed out of wetlands more slowly and begins to accumulate, resulting in more available N for plant uptake. *Phragmites* is an opportunistic invader capable of outcompeting natives for this available N, growing taller, and shading out neighboring plants (Mozdzer and Zieman 2010, Holdredge and Bertness 2011). Under shorter RT_h, N is quickly flushed from wetlands, reducing available N and preventing rapid *Phragmites* growth and shading of natives (Borin and Tocchetto 2007). However, when N loading exceeded 15 g N m^{-2} y^{-1} even the shortest RT_h we simulated (1 day) cannot prevent *Phragmites* from invading and dominating wetland communities. This suggests that invasion is most sensitive to changes in RT_h in wetlands receiving low inputs of N.

Typha invasion was similarly successful under lower N loading regimes as RT_h lengthened. However, at higher levels of N loading, *Typha* invasion success declined for all RT_h scenarios except the shortest (1 day; Appendix S1: Fig. S2). This outcome is likely due to the robust productivity of natives under high N loads or increased ecosystem N as a result of longer RT_h. As natives grow and reproduce quickly with abundant N in the 15 years prior to invader introduction, the community is effectively able to prevent *Typha* from invading. We tested this explanation by performing a small set of diagnostic simulations. By increasing *Typha* propagule pressure (65 individuals in a cohort rather than 15) and introducing *Typha* with the native community at year one before the natives can fill the model space, *Typha* was able to dominate the community under high N loading and long RT_h scenarios that it failed to invade if introduced in year 15 (Appendix S1: Fig. S3). This indicates that *Typha* establishment was indeed prevented by the rapid expansion and productivity of the native community, particularly by the larger native, *Schoenoplectus acutus,* which can grow up to 3m tall (Gleason and Cronquist 1991). This has been further demonstrated in arid grasslands, where diverse native communities exhibited high resistance to invasion by exotic knapweed, even with abundant available resources thought to facilitate the invader (Maron and Marler 2007). We believe this response was unique to *Typha*, and not observed in *Phragmites* invasion scenarios, because of their differences in physiology and morphology. Compared to *Typha, Phragmites* has a higher relative growth rate, maximum size, and leaf architecture that more completely shades neighboring plants, allowing it to outcompete even the densest stand of natives (Martina et al. 2016).

Conclusions

Reducing nutrient loads downstream and controlling invasive species are both common management objectives and we found that optimizing one may come at the cost of the other. Optimizing management to mitigate negative outcomes is practical in wetlands where hydrology and RT_h can be directly controlled, like tertiary treatment wetland or waterfowl impoundments (Winton et al. 2016). The simulations we present are modeled after coastal wetlands of the Great Lakes, where controlling hydrology is more difficult and occurs less often (Wilcox 1993). Process-based simulation models, like Mondrian, provide needed insight into functions governed by complex interactions of drivers, including hydrology and nutrient loading, which would be difficult to infer from field studies. In Great Lakes wetlands RT_h is modulated by multi-year

609 water level fluctuations that determine the direction and rate of water flow in river mouths and
610 along coastlines. With accurate predictions of lake levels, practitioners can anticipate changes in
611 RT_h and subsequent shifts in N removal services and wetland invasibility. For example, when
612 lake levels are high, the hydrologic gradient from coastal wetlands to the lake is shallower,
613 wetland water outflow is slower, and RT_h is longer. In these scenarios management strategies
614 should focus on invasion threats as longer that results from high lake level will facilitate greater
615 N removal, reducing the need for intervention. When lake levels are lower, priorities should shift
616 to reducing N loading into wetlands, when ideal conditions for N removal decline as downslope
617 hydrologic gradients increase, RT_h shortens, and invasion resistance increases, particularly
618 wetlands receiving ≤15 g N m^{-2} y^{-1} where changes in RT_h can be a determining factor of wetland
619 invasibility.
620 These results can provide timely guidance in the management of both N delivery to the
621 Great Lakes and invasion of vulnerable coastal wetlands as Great Lakes watersheds continue to
622 deliver high amounts of N (Choquette et al. 2019) and lakes experience record-breaking water
623 levels (Gronewold and Rood 2019). By combining lake level predictions with our understanding
624 of invasive species propagation and land use change impacts on watershed nutrient transport we
625 can prioritize intervention in wetlands most vulnerable to change while optimizing those with
626 high potential for service provisioning. Although our results are specific to Great Lakes coastal
627 wetlands, these trends and tradeoffs are general enough to be applied to other freshwater coastal
628 wetlands with similar seasonal hydrology and climate. Furthermore, Mondrian's ability to
629 simulate complex mechanisms shared among temperate herbaceous wetlands throughout time
630 and across regions gives practitioners freedom to explore scenario-specific management
631 strategies by simply defining the environmental setting (e.g. climate patterns, hydrology, and
632 plant communities). This control allows users to fine-tune model predictions to seasonal timing
633 of N delivery, anticipated shifts in seasonal hydrology patterns, including timing of high water,
634 and climate change impacts on wetland biota to further enhance our understanding of the future
635 and function of important and vulnerable coastal wetlands.
636
637
638 ACKNOWLEDGMENTS

We thank Anthony Kendall, Sherry Martin, and Luwen Wan at Michigan State University Hydrogeology Lab for providing analysis of instream nutrient data. Funding for this work was provided by NASA IDS Grant #80NSSC17K0262.

SUPPORTING INFORMATION

Additional supporting information may be found online at: [link to be added in production].

DATA AVAILABILITY

Data are available from the Deep Blue repository at the University of Michigan (Sharp 2020): https://doi.org/10.7302/thef-4p55

References

Alldred, M., and S. B. Baines. 2016. Effects of wetland plants on denitrification rates: a meta-analysis. Ecological Applications 26:676–685.

Bansal, S., S. C. Lishawa, S. Newman, B. A. Tangen, D. Wilcox, D. Albert, M. J. Anteau, M. J. Chimney, R. L. Cressey, E. DeKeyser, K. J. Elgersma, S. A. Finkelstein, J. Freeland, R. Grosshans, P. E. Klug, D. J. Larkin, B. A. Lawrence, G. Linz, J. Marburger, G. Noe, C. Otto, N. Reo, J. Richards, C. Richardson, L. R. Rodgers, A. J. Schrank, D. Svedarsky, S. Travis, N. Tuchman, and L. Windham-Myers. 2019. *Typha* (Cattail) invasion in North American wetlands: Biology, regional problems, impacts, ecosystem services, and management. Wetlands 39:645–684.

Barton, K. 2019. MuMIn: Multi-Model Inference. R package version 1.43.15.

Bates, D., M. Martin, B. Bolker, and S. Walker. 2015. Fitting linear-effects models using lme4. Journal of Statistical Software 67:1–48.

Bellinger, B. J., T. M. Jicha, L. P. Lehto, L. R. Seifert-Monson, D. W. Bolgrien, M. A. Starry, T. R. Angradi, M. S. Pearson, C. Elonen, and B. H. Hill. 2014. Sediment nitrification and denitrification in a Lake Superior estuary. Journal of Great Lakes Research 40:392–403.

Bremner, J. M., and K. Shaw. 1958. Denitrification in soil. II. Factors affecting denitrification. The Journal of Agricultural Science 51:40–52.

Burnham, K. P., and D. R. Anderson. 2002. Model selection and multimodel inference : a

practical information-theoretic approach. Second edition. Springer, New York, New York.

Chanton, J. P., and G. J. Whiting. 1996. Methane stable isotopic distributions as indicators of gas transport mechanisms in emergent aquatic plants. Aquatic Botany 54:227–236.

Corenblit, D., A. C. W. Baas, G. Bornette, J. Darrozes, S. Delmotte, R. A. Francis, A. M. Gurnell, F. Julien, R. J. Naiman, and J. Steiger. 2011. Feedbacks between geomorphology and biota controlling Earth surface processes and landforms: A review of foundation concepts and current understandings. Earth-Science Reviews 106:307–331.

Currie, W. S., D. E. Goldberg, J. Martina, R. Wildova, E. Farrer, and K. J. Elgersma. 2014. Emergence of nutrient-cycling feedbacks related to plant size and invasion success in a wetland community-ecosystem model. Ecological Modelling 282:69–82.

Dettmann, E. H. 2007. Effect of water residence time on annual export and denitrification of nitrogen in estuaries: A model analysis. Estuaries 24:481.

Diaz, R. J., and R. Rosenberg. 2008. Spreading dead zones and consequences for marine ecosystems. Science (New York, N.Y.) 321:926–9.

Ehrenfeld, J. G. 2003. Effects of exotic plant invasions on soil nutrient cycling processes. Ecosystems 6:503–523.

Elgersma, K. J., J. P. Martina, D. E. Goldberg, and W. S. Currie. 2017. Effectiveness of cattail (*Typha* spp.) management techniques depends on exogenous nitrogen inputs. Elem Sci Anth 5:19.

Erwin, K. L. 2009. Wetlands and global climate change: the role of wetland restoration in a changing world. Wetlands Ecology and Management 17:71–84.

Findlay, S., P. Groffman, and S. Dye. 2003. Effects of *Phragmites australis* removal on marsh nutrient cycling. Wetlands Ecology and Management 11:157–165.

Goldberg, D. E., J. P. Martina, K. J. Elgersma, and W. S. Currie. 2017. Plant size and competitive dynamics along nutrient gradients. The American Naturalist 190:229–243.

Hamlin, Q. F., A. D. Kendall, S. L. Martin, H. D. Whitenack, J. A. Roush, B. A. Hannah, and D. W. Hyndman. 2020. Quantifying landscape nutrient inputs with spatially explicit nutrient

source estimate maps. Journal of Geophysical Research: Biogeosciences 125.

Han, H., J. D. Allan, and D. Scavia. 2009. Influence of climate and human activities on the relationship between watershed nitrogen input and river export. Environmental Science and Technology 43:1916–1922.

Hansson, L., C. Bronmark, P. Anders Nilsson, and K. Abjornsson. 2005. Conflicting demands on wetland ecosystem services: nutrient retention, biodiversity or both? Freshwater Biology 50:705–714.

Hernandez, M. E., and W. J. Mitsch. 2007. Denitrification in created riverine wetlands: Influence of hydrology and season. Ecological Engineering 30:78–88.

Hoagland, P., D. M. Anderson, Y. Kaoru, and A. W. White. 2002. The economic effects of harmful algal blooms in the United States: Estimates, assessment issues, and information needs. Estuaries 25:819–837.

Howarth, R. W., A. Sharpley, and D. Walker. 2002. Sources of nutrient pollution to coastal waters in the United States: Implications for achieving coastal water quality goals. Estuaries 25:656–676.

Ishida, C. K., J. J. Kelly, and K. A. Gray. 2006. Effects of variable hydroperiods and water level fluctuations on denitrification capacity, nitrate removal, and benthic-microbial community structure in constructed wetlands. Ecological Engineering 28:363–373.

Jessop, J., G. Spyreas, G. E. Pociask, T. J. Benson, M. P. Ward, A. D. Kent, and J. W. Matthews. 2015. Tradeoffs among ecosystem services in restored wetlands. Biological Conservation 191:341–348.

Jordan, S. J., J. Stoffer, J. A. Nestlerode, and J. A. Nestlerode. 2015. Wetlands as sinks for reactive nitrogen at continental and global scales: A meta-analysis. Ecosystems 14:144–155.

Kadlec, R. H., and S. Wallace. 1997. Treatment Wetlands. Page Journal of Environmental Quality. CRC Press.

Keough, J. R., T. A. Thompson, G. R. Guntenspergen, and D. A. Wilcox. 1999. Hydrogeomorphic factors and ecosystem responses in coastal wetlands of the Great Lakes.

722 Wetlands 19:821–834.

723 Kirk, G. J. D., and H. J. Kronzucker. 2005. The potential for nitrification and nitrate uptake in
724 the rhizosphere of wetland plants: A modelling study. Annals of Botany 96:639–646.

725 Kjellin, J., S. Hallin, and A. Wörman. 2007. Spatial variations in denitrification activity in
726 wetland sediments explained by hydrology and denitrifying community structure. Water
727 Research 41:4710–4720.

728 Knox, A. K., R. A. Dahlgren, K. W. Tate, and E. R. Atwill. 2008. Efficacy of natural wetlands to
729 retain nutrient, sediment and microbial pollutants. Journal of Environment Quality 37:1837.

730 Krieger, K. A. 2003. Effectiveness of a coastal wetland in reducing pollution of a Laurentian
731 Great Lake: Hydrology, sediment, and nutrients. Wetlands 23:778–791.

732 Kröger, R., M. T. Moore, M. A. Locke, R. W. Steinriede, R. F. Cullum, C. T. Bryant, S. Testa,
733 and C. M. Cooper. 2009. Evaluating the influence of wetland vegetation on chemical
734 residence time in Mississippi Delta drainage ditches. Agricultural Water Management
735 96:1175–1179.

736 Lapointe, B. E., L. W. Herren, D. D. Debortoli, and M. A. Vogel. 2015. Evidence of sewage-
737 driven eutrophication and harmful algal blooms in Florida's Indian River Lagoon. Harmful
738 Algae 43:82–102.

739 Lishawa, S. C., K. J. Jankowski, P. Geddes, D. J. Larkin, A. M. Monks, and N. C. Tuchman.
740 2014. Denitrification in a Laurentian Great Lakes coastal wetland invaded by hybrid cattail
741 (*Typha* × *glauca*). Aquatic Sciences 76:483–495.

742 Martina, J. P., W. S. Currie, D. E. Goldberg, and K. J. Elgersma. 2016. Nitrogen loading leads to
743 increased carbon accretion in both invaded and uninvaded coastal wetlands. Ecosphere 7:1–
744 19.

745 McCarthy, M. J., W. S. Gardner, P. J. Lavrentyev, K. M. Moats, F. J. Jochem, and D. M. Klarer.
746 2008. Effects of hydrological flow regime on sediment-water interface and water column
747 nitrogen dynamics in a Great Lakes coastal wetland (Old Woman Creek, Lake Erie).
748 Journal of Great Lakes Research 33:219–231.

749 Michalak, A. M., E. J. Anderson, D. Beletsky, S. Boland, N. S. Bosch, T. B. Bridgeman, J. D.
750 Chaffin, K. Cho, R. Confesor, I. Daloglu, J. V Depinto, M. A. Evans, G. L. Fahnenstiel, L.
751 He, J. C. Ho, L. Jenkins, T. H. Johengen, K. C. Kuo, E. Laporte, X. Liu, M. R. McWilliams,
752 M. R. Moore, D. J. Posselt, R. P. Richards, D. Scavia, A. L. Steiner, E. Verhamme, D. M.
753 Wright, and M. A. Zagorski. 2013. Record-setting algal bloom in Lake Erie caused by
754 agricultural and meteorological trends consistent with expected future conditions.
755 Proceedings of the National Academy of Sciences of the United States of America
756 110:6448–52.

757 Parton, W. J., A. R. Mosier, D. S. Ojima, D. W. Valentine, D. S. Schime, K. Weier, and A. E.
758 Kulmala. 1996. Generalized model for N_2 and N_2O production from nitrification and
759 denitrification. Global Biogeochemical Cycles 10:401–412.

760 Perez, B. C., J. W. Day, D. Justic, R. R. Lane, and R. R. Twilley. 2011. Nutrient stoichiometry,
761 freshwater residence time, and nutrient retention in a river-dominated estuary in the
762 Mississippi delta. Hydrobiologia 658:41–54.

763 Pezeshki, S. R. 2001. Wetland plant responses to soil flooding. Environmental and Experimental
764 Botany 46:299–312.

765 Piña-Ochoa, E., and M. Álvarez-Cobelas. 2006. Denitrification in aquatic environments: A
766 cross-system analysis. Biogeochemistry 81:111–130.

767 R Core Team. 2019. R: A language and environment for statistical computing. R Foundation for
768 Statistical Computing, Vienna, Austria.

769 Reddy, K. R., W. H. Patrick, and C. W. Lindau. 1989. Nitrification-denitrification at the plant
770 root-sediment interface in wetlands. Limnology and Oceanography 34:1004–1013.

771 Reed, D., and D. Cahoon. 1992. The relationship between marsh surface topography,
772 hydroperiod, and growth of Spartina alterniflora in a deteriorating Louisiana salt marsh.
773 Journal of Coastal Research 8:77–87.

774 Rickey, M. A., and R. C. Anderson. 2004. Effects of nitrogen addition on the invasive grass
775 *Phragmites australis* and a native competitor *Spartina pectinata*. Journal of Applied
776 Ecology 41:888–896.

Sánchez-Carrillo, S., D. G. Angeler, R. Sánchez-Andrés, M. Alvarez-Cobelas, and J. Garatuza-Payán. 2004. Evapotranspiration in semi-arid wetlands: Relationships between inundation and the macrophyte-cover:open-water ratio. Advances in Water Resources 27:643–655.

Saunders, D. L., and J. Kalff. 2001. Nitrogen retention in wetlands, lakes and rivers. Hydrobiologia 443:205–212.

Sharp, S. 2020. Hydrologic flushing rates drive nitrogen cycling and plant invasion in a freshwater coastal wetland model Ecological Applications EAP20-0253 Reproducable Data Archive. Data set. University of Michigan - Deep Blue. https://doi.org/10.7302/thef-4p55

Tylova-Munzarova, E., B. Lorenzen, H. Brix, and O. Votrubova. 2005. The effects of NH_4^+ and NO_3^- on growth, resource allocation and nitrogen uptake kinetics of *Phragmites australis* and *Glyceria maxima*. Aquatic Botany 81:326–342.

Uddin, M. N., and R. W. Robinson. 2017. Responses of plant species diversity and soil physical-chemical-microbial properties to *Phragmites australis* invasion along a density gradient. Scientific Reports 7:11007.

Vymazal, J. 2007. Removal of nutrients in various types of constructed wetlands. Science of the Total Environment 380:48–65.

Weltzin, J. F., J. K. Keller, S. D. Bridgham, J. Pastor, P. B. Allen, and J. Chen. 2005. Litter controls plant community composition in a northern fen. Oikos 110:537–546.

Wilcox, D. A. 2012. Response of wetland vegetation to the post-1986 decrease in Lake St. Clair water levels: Seed-bank emergence and beginnings of the *Phragmites australis* invasion. Journal of Great Lakes Research 38:270–277.

Windham, L., and L. A. Meyerson. 2003. Effects of common reed (*Phragmites australis*) expansions on nitrogen dynamics of tidal marshes of the northeastern U.S. Estuaries 26:452–464.

Xue, Y., D. A. Kovacic, M. B. David, L. E. Gentry, R. L. Mulvaney, and C. W. Lindau. 1999. In situ measurements of denitrification in constructed wetlands. Journal of Environment Quality 28:263.

805 Zedler, J. B., and S. Kercher. 2004. Causes and consequences of invasive plants in wetlands:
806 Opportunities, opportunists, and outcomes. Critical Reviews in Plant Sciences 23:431–452.

807

Table 1. List of sites, empirical field data, and Mondrian model output and input values used to determine scaling parameters and calibrate denitrification in Mondrian. Mondrian was calibrated using empirical values of annual average denitrification, biomass, nitrogen inputs (NH_4^+-N and NO_3^--N), water depth, and hydrologic residence time (RT_h).

	Empirical values		Model output		Model input				
Site	Denitrification (g N m^{-2} y^{-1})	Biomass (g C m^{-2})	Denitrification (g N m^{-2} y^{-1})	Biomass (g C m^{-2})	NH_4^+ (g N m^{-2} y^{-1})	NO_3^- (g N m^{-2} y^{-1})	Water depth (cm)	RT_h (days)	Citation
Old Woman Creek, OH	10.6	*No data*	9.3	494	50.2	228	0±100	4.2	McCarthy et al. 2008
Champaign, IL	10.0	500	11.9	494	36.0	144	16±25	7.0	Xue et al. 1999
St Louis Bay Estuary, MN	5.7	157	0.3	267	0.0	10.8	75±0	13.0	Bellinger et al. 2014
Olentangy River, Columbus, OH	2.7	779	1.2	624	24.5	98.1	-2±40	1.0	Hernandez and Mitsch 2007
Cheboygan Marsh, MI	0.7	591	0.3	281	0.0	12.9	4±6	3.2	Lishawa et al. 2014

Table 2. Predictor variables and their various factor levels used in model simulations for this study. Each predictor variable was crossed in a semi-factorial manner with the other drivers (i.e. $RT_h = f$[water level] was not crossed with constant hydroperiod resulting in n=1380 unique treatment combinations). RT_h = hydrologic residence time (days).

N loading (g N m^{-2} y^{-1})	NH_4^+-N:NO_3^--N mass ratio	RT_h (days)	Hydroperiod	Plant invader identity
1	0:1	*f*(water level)	Constant 15cm	*Phragmites australis*
5	1:7.3	1	Constant -15cm	*Phragmites australis*
10	1:3	10	Weekly (±50cm)	*Typha x glauca*
15	4:1	100	Monthly (±50cm)	
30	1:0	365	Semi-annual (±50cm)	
100				

Table 3. Values of the differences (Δ) in AIC (Akaike Information Criterion) between each Generalized Linear Mixed Model (GLMM) relative to the best model (in **bold**) of four response variables: annual N removal, percent of N inflow denitrified, N removal efficiency, and invader percent of total NPP. Model variables include annual N loading (*N Load*), N-species ratio (*N ratio*), hydrologic residence time (RT_h), hydroperiod (*Hydro*), and invader species identity (*Invader*). Included model terms selected base on a forward stepwise selection process. Interaction terms include all lower order interactions and main effects (e.g. 3-way interaction includes the 3 main effects and possible 2-way interactions). P<0.001 for all models.

Variable	Model equation	df	ΔAIC	Adj. R^2
Annual N removal	$a = N\ load \times RT_h \times Hydro$	149	355	0.95
	$b = a + (N\ load \times Hydro \times N\ ratio)$	474	37	0.96
	$c = b + (N\ load \times RT_h \times N\ ratio)$	624	13	0.96
	$c + (N\ load \times RT_h \times Invader)$	**684**	**0**	**0.96**

N removal efficiency	$a = (Hydro \times RT_h) + (Hydro \times N\ load)$	54	97	0.83
	$b = a + (N\ load \times Invader)$	66	91	0.83
	$b + (N\ load \times RT_h \times Hydro)$	**161**	**0**	**0.84**
% N denitrified	$a = N\ load \times RT_h \times Hydro$	149	39	0.83
	$b = a + (N\ ratio \times N\ load)$	179	9	0.83
	$c = b + (N\ ratio \times Hydro)$	209	4	0.83
	$c + (N\ ratio \times RT_h)$	**234**	**0**	**0.83**
Invader % of total NPP	$a = N\ load \times RT_h \times Invader$	59	1	0.31
	$a + (RT_h \times Hydro)$	**85**	**0**	**0.32**

Table 4. Relative variable importance (RVI) values of all main effects, 2-way, and 3-way interactions of predictor variables used in best fit GLMM models. The highest RVI values within each order (main effect or interactions) of each response variable are in **bold**, representing the terms we discuss in this study**.** Note that RVI is a relative value such that the RVI of main effects and interaction terms can only be compared to similar order terms (e.g. a main effect can be compared to another main effect, but not to any interaction term).

		Annual N removal	*N removal efficiciency*	*% N denitrified*	*Invader % of total NPP*
Main effect	RT_h	**1.00**	**1.00**	**1.00**	**1.00**
	Hydro	**1.00**	**1.00**	**1.00**	0.99
	N load	**1.00**	**1.00**	**1.00**	**1.00**
	N ratio	0.08	0.21	0.29	0.02
	Invader	0.51	0.54	0.66	**1.00**
2-way interactions	$RT_h \times Hydro$	**1.00**	**0.99**	**0.99**	0.65
	$RT_h \times N\ load$	**1.00**	0.58	**0.99**	**0.99**
	$RT_h \times N\ ratio$	0.10	0.03	0.62	0.00

	RT_h × Invader	0.36	0.34	0.27	**0.99**
	N load × Hydro	**1.00**	**0.99**	**0.99**	0.26
	N load × N ratio	**1.00**	0.30	0.89	0.00
	N load × Invader	**1.00**	0.90	0.42	**0.99**
	Hydro × N ratio	0.00	0.00	0.08	0.00
3-way interactions	*N load × RT_h × Hydro*	**1.00**	**0.99**	**0.99**	0.00
	N load × RT_h × N ratio	**1.00**	0.00	0.08	0.00
	N load × RT_h × Invader	0.99	0.00	0.51	**0.72**
	N load × Hydro × N ratio	**1.00**	0.91	0.01	0.00

Figure 1. Conceptual model depicting the influence of various biotic and abiotic drivers on wetland N availability and invasion success of wetland macrophytes. Blue boxes represent larger storages or processes while orange ovals represent smaller processes that occur within the larger blue boxes. Wetland N pool includes inorganic NO_3^--N and NH_4-N as well as litter and soil organic N. Solid lines represent direct effects and dashed lines represent indirect effects. H_1, H_2, and H_3 boxes represent hypotheses predicting effects of water residence time, hydroperiod, and plant invasions on N cycling.

Figure 2. Observed and simulated values of denitrification from 5 regional sentinel sites used for Mondrian calibration of ecosystem-level scaling parameters. Diagonal line represents hypothetical 1:1 relationship of predicted model and observed field data.

Figure 3. Annual nitrogen (N) removal ± S.E. as a function of water residence time (RT_h, plotted on a log scale) in simulations of weekly (left panels) and semi-annual and permanent (labeled as semi-annual; right panels) flooding regimes. Each row of panels corresponds to a different level of wetland N inflow in g N m^{-2} y^{-1}. Larger circles represent greater percentage (%) of invader NPP relative to total community NPP. Points on the x axis that fall between 1 and 10 days represent treatments where residence time was a function of water level with an annual average water residence time of ca. 4 days.

Figure 4. Annual nitrogen (N) removal across a range of NH_4^+-N:NO_3^--N ratios. Ratios of 1:7.3, 1:3, and 4:1 reflect watershed N inputs for urban, high-intensity agriculture, and rural land use

854 classes, respectively. Ratios of 0:1 and 1:0 represent hypothetical ammonium-only and nitrate-
855 only N loading, respectively. Bar colors represent water residence time (RT_h).
856
857 Figure 5. Plant available inorganic N (IN; NH_4^+-N + NO_3^--N), plant IN uptake, and total organic
858 N (ON) in soil pools as a function of N loading in simulations of weekly (left panels) and semi-
859 annual and permanent (labeled as semi-annual; right panels) flooding regimes. Bar colors
860 represent water residence time (RT_h).
861 Figure 6. Nitrogen (N) removal efficiency (N_{rem}/ N_{in}) ± S.E. as a function of water residence time
862 (RT_h, plotted on a log scale) in simulations of weekly (left panels) and semi-annual and
863 permanent (labeled as semi-annual; right panels) flooding regimes. Each row of panels
864 corresponds to a different level of wetland N inflow in g N m^{-2} y^{-1}. Larger circles represent
865 greater percentage (%) of invader NPP relative to total community NPP. Points on the x axis that
866 fall between 1 and 10 days represent treatments where residence time was a function of water
867 level with an annual average water residence time of ca. 4 days.
868 Figure 7. Percentage (%) ± S.E. of available N from N_{inflow} that is denitrified on an annual basis
869 as a function of water residence time (RT_h, plotted on a log scale) in simulations of weekly (left
870 panels) and semi-annual and permanent (labeled as semi-annual; right panels) flooding regimes.
871 Each row of panels corresponds to a different level of wetland N inflow in g N m^{-2} y^{-1}. Larger
872 circles represent greater percentage (%) of invader NPP relative to total community NPP. Points
873 on the x axis that fall between 1 and 10 days represent treatments where residence time was a
874 function of water level with an annual average water residence time of ca. 4 days.

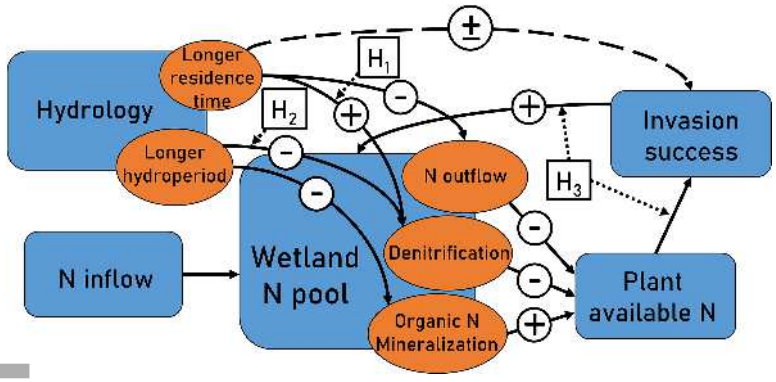

eap_2233_f1.tif

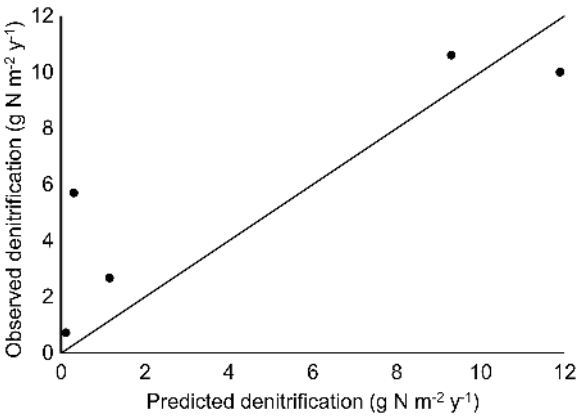

eap_2233_f2.tif

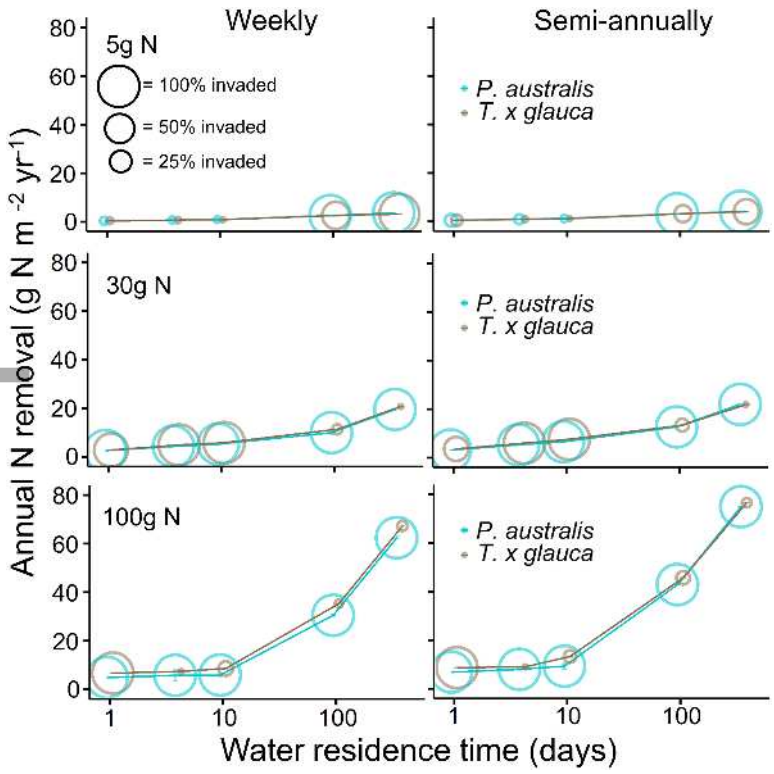

eap_2233_f3.tif

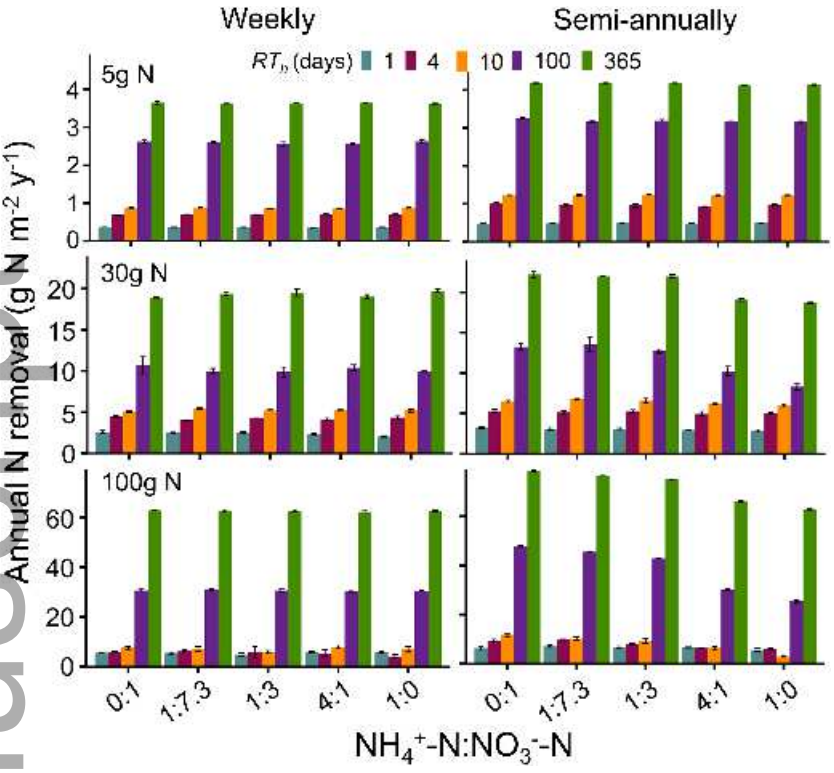

eap_2233_f4.tif

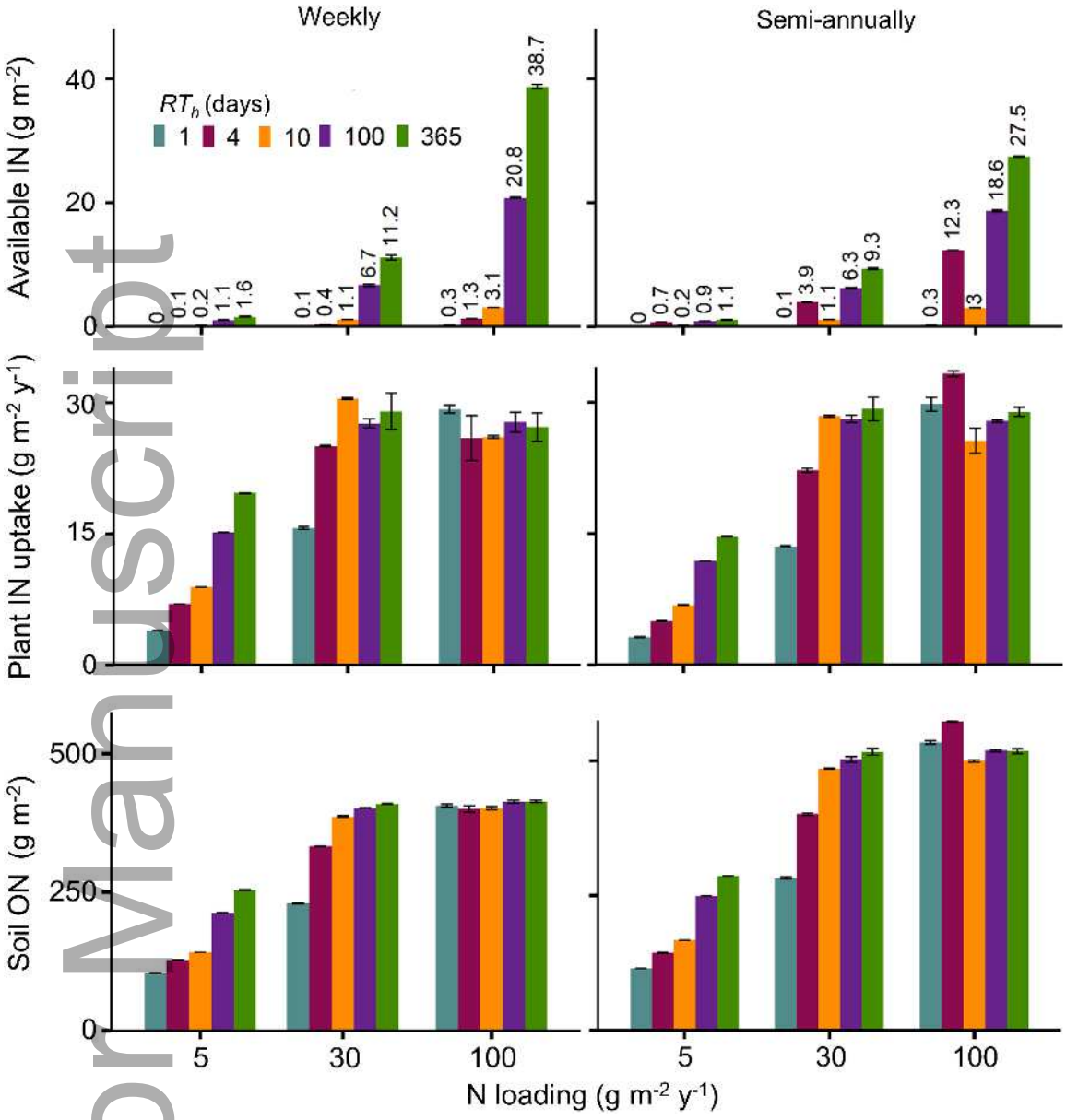

eap_2233_f5.tif

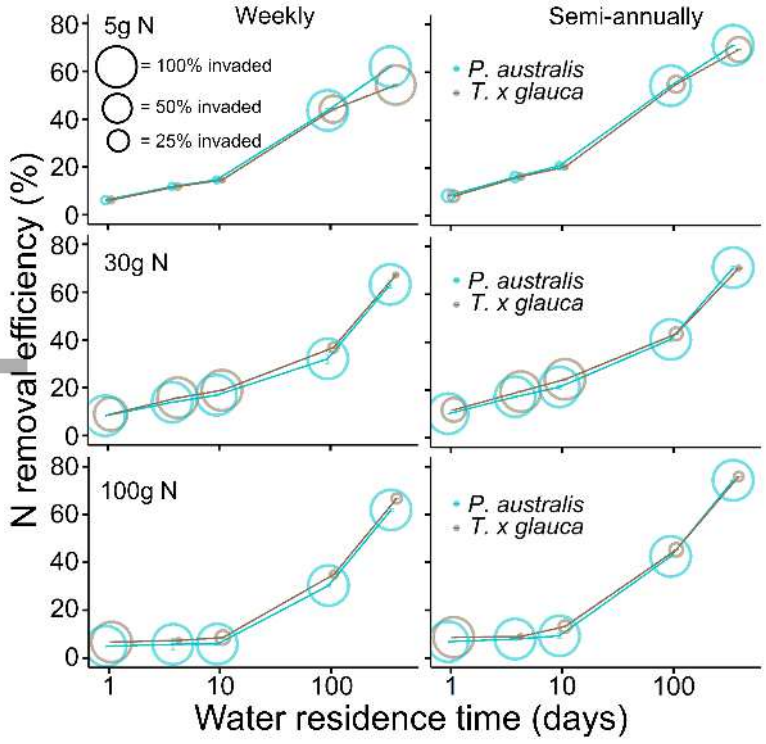

eap_2233_f6.tif

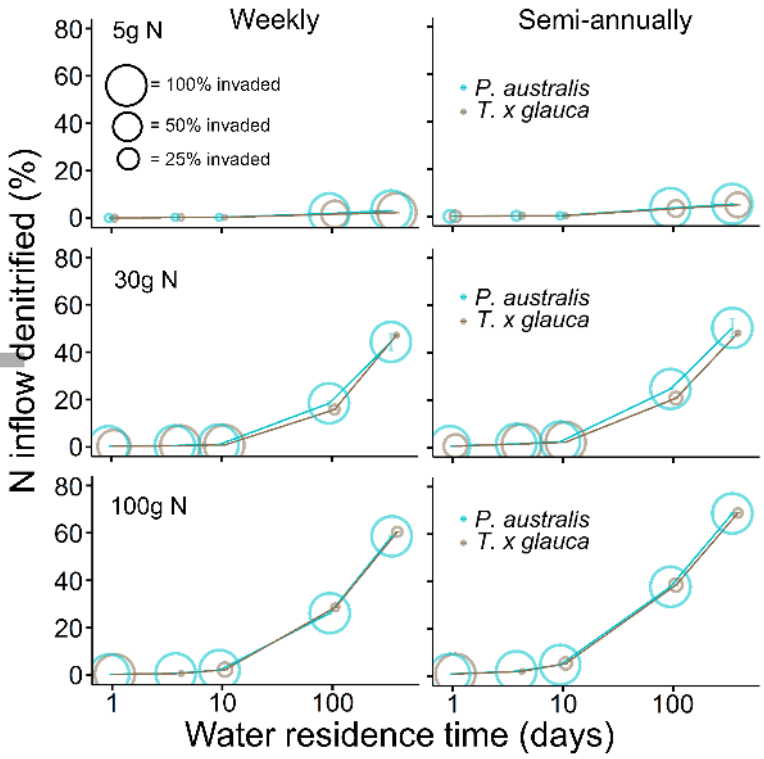

eap_2233_f7.tif